

1 **Intermittent structural weakening and acceleration of the Thwaites Glacier Tongue**  
2 **between 2000 and 2018.**

3  
4 B.W.J. Miles<sup>1\*</sup>, C.R. Stokes<sup>1</sup>, A. Jenkins<sup>2,3</sup>, J.R. Jordan<sup>2</sup>, S.S.R. Jamieson<sup>1</sup>, G.H.  
5 Gudmundsson<sup>2</sup>

6  
7 <sup>1</sup>Department of Geography, Durham University, Durham, DH1 3LE, UK

8 <sup>2</sup>Department of Geography and Environmental Sciences, Northumbria University, Newcastle upon Tyne, NE1  
9 8ST, UK

10 <sup>3</sup>British Antarctic Survey, Natural Environment Research Council, Cambridge, UK

11 \*Correspondence to: a.w.j.miles@durham.ac.uk  
12  
13

14 **Abstract** Evolving conditions at the terminus of Thwaites Glacier will be important in  
15 determining the rate of its future sea-level contribution over the coming decades. Here, we  
16 use remote sensing observations to investigate recent changes (2000-2018) in the structure  
17 and velocity of Thwaites Glacier and its floating tongue. We show that the main trunk of  
18 Thwaites Glacier has accelerated by 38% over this period, whilst its previously intact floating  
19 tongue has transitioned to a weaker mélange of fractured icebergs bounded by sea-ice.  
20 However, the rate of structural weakening and acceleration were not uniform across the  
21 observational period and we identify two periods of rapid acceleration and structural  
22 weakening (2006-2012; 2016-2018), separated by a period of deceleration and re-advance of  
23 the structurally-intact shear margin boundary (2012-2015). The timing of these  
24 accelerations/decelerations strongly suggest a link to variable ocean forcing. The weakened  
25 tongue now has some dependency on landfast sea ice for structural integrity and is vulnerable  
26 to changes in landfast ice persistency. Future reductions in landfast sea-ice could manifest  
27 from changes in climate and/or the imminent removal of the B-22A iceberg from the  
28 Thwaites embayment. Such changes could have important implications for the integrity of the  
29 ice tongue and future glacier discharge.  
30  
31

32 **1. Introduction**  
33

34 Observations have shown that the Amundsen Sea Sector of the West Antarctic Ice Sheet  
35 (WAIS) is currently losing mass at a greater rate than anywhere else in Antarctica (Shepherd  
36 and others, 2018; Rignot and others, 2019). Ice shelves in the region have been rapidly  
37 thinning (Paolo and others, 2015) and ice discharge has increased 77% between 1973 and  
38 2014 (Mouginot and others, 2014), resulting in inland thinning and grounding line retreat  
39 (McMillan and others, 2014; Konrad and others, 2018; Milillo and others, 2019). These  
40 changes are thought to be in response to periodic intrusions of warm Circumpolar Deep  
41 Water that increase basal melt rates beneath ice shelves and ice tongue (Thoma and others,  
42 2008; Jenkins and others, 2010; 2018).

43

44 Whilst the present day mass loss of the Amundsen Sea Sector is of significant concern, there  
45 is a potential for a much higher rate of mass loss in the near-future (Golledge and others,  
46 2015; DeConto and Pollard, 2016). Of particular concern is the Thwaites Glacier Catchment,  
47 which holds enough ice to raise global mean sea level by 59 cm (Holt and others, 2006) and,  
48 together with adjacent catchments, the West Antarctic Ice Sheet holds enough ice to raise  
49 global mean sea level by more than 3 m (Scambos and others, 2017). As most of the ice in  
50 the Thwaites catchment is grounded on bedrock that lies below sea level and that deepens  
51 inland (Fretwell and others, 2013), there is potential for marine ice sheet instability to  
52 accelerate mass loss beyond that which might be expected from external forcing alone  
53 (Mercer, 1978; Schoof, 2007), unless ice shelves provide a sufficient amount of buttressing  
54 (e.g. Gudmundsson and others, 2012; Gudmundsson, 2013; Gudmundsson and others, 2019).  
55 Indeed, some numerical models (Joughin and others, 2014; Seroussi and others, 2017) and  
56 observations (Rignot and others 2014) have raised the possibility that the early-onset of this  
57 irreversible process may already be underway in the Thwaites Basin. If floating ice shelves  
58 are lost at some point during this process, resulting in the formation of unstable ice cliffs,  
59 there is potential for much higher rates of mass loss (DeConto and Pollard, 2016). However,  
60 at present, there are very few observations to constrain this process and it may not be required  
61 to explain past changes in sea level from Antarctic ice loss (Edwards and others, 2019).

62

63 Given the above, it is clear that the evolving conditions at the ice front of Thwaites Glacier  
64 are likely to be an important control on the rates and timing of future sea level contributions  
65 (e.g. Scambos and others, 2017). In this paper, we use satellite imagery to investigate the  
66 changes in structure of the Thwaites Glacier Tongue over the past 18 years (2000 to 2018).  
67 We analyse how the observed changes in structure relate to changes in both its calving

68 pattern and its velocity, and then discuss the observed changes in relation to the near-future  
69 evolution of Thwaites Glacier.

70

## 71 **2. Data and Methods**

### 72 **2.1 Ice-front positions 2000-2018: MODIS**

73

74 We measured annual changes in the ice-front position and velocity of Thwaites Glacier,  
75 extending the observations from MacGregor and others (2012), which spanned the period  
76 1972 to 2011. We digitized ice-front positions using MODIS imagery, obtained from the  
77 NASA WorldView application, and acquired every March from 2000 to 2018 (Dataset S1).  
78 In some cases, the heavily fractured nature of the Thwaites Glacier Tongue made mapping  
79 the ice front difficult. For consistency, we took the same approach for each image and always  
80 mapped the outer edge of connected ice blocks at each time step (Fig. S1). Changes in ice-  
81 front position were quantified using the box method, which takes into account uneven  
82 changes along the ice front (Moon and Joughin, 2008; Miles and others, 2016).

83

### 84 **2.2. Annual velocity fields (2000-2017)**

85

86 Velocity fields from 2000 and 2002 were obtained from Mouginot and others (2014). These  
87 datasets were processed using Radarsat-1 data from the austral winter and are available at a  
88 spatial resolution of 450 m, with errors of  $\pm 5 \text{ m yr}^{-1}$  (Mouginot and others, 2014). Annual  
89 velocity fields between 2005-2006 and 2016-2017 were obtained from the MEaSURES  
90 dataset (Mouginot and others, 2017). These products are derived from the stacking of  
91 multiple velocity fields derived from a variety of sensors between July and June in the  
92 following year, and are available at 1 km spatial resolution. Errors in these products are  
93 estimated by a combination of the standard deviation and count of scenes and vary from year  
94 to year (Mouginot and others, 2017). For simplicity we assume the error to be the largest  
95 error estimate ( $\pm 32 \text{ m yr}^{-1}$ ) for all years.

96

### 97 **2.3 Sub-annual velocity fields (2013-2018): Landsat-8 and Sentinel-1**

98

99 In addition to the annual velocity datasets described above, we also used Landsat-8 and  
100 Sentinel-1 satellites for ice velocity measurements at a higher temporal resolution (16 days  
101 and 6/12 days, respectively). We used the pre-computed raw Landsat-8-derived velocity

102 fields available from the GoLive dataset (Fahnestock and others, 2016), that are available at a  
103 600 m spatial resolution from November 2013 onwards. To maximise temporal coverage, we  
104 used all six Landsat-8 scenes which cover Thwaites Glacier and include all velocity fields  
105 generated from image pairs separated by 16, 32 and 48 days (Dataset S1). The raw velocity  
106 fields were post-processed to improve their overall quality. This was done by removing pixels  
107 that had the following properties: (i) peak correlation values below a threshold of the  
108 normalized cross-correlation algorithm from the GoLive workflow of less than 0.3; or (ii)  
109 values outside the range of  $\pm 50\%$  of the MEaSURES velocity product. Once these pixels were  
110 removed, the final velocity product was computed by applying a 3x3 low pass filter.

111

112 For Sentinel-1 data we used an automated workflow from the European Space Agency  
113 Sentinel Application Platform (SNAP) to compute velocity fields. We first download  
114 Interferometric Wide Swath (IW) Ground Range Detected (GRD) images from the  
115 Copernicus Sentinel Hub before applying precise orbits and calibration. These images have  
116 been consistently available over Thwaites since late 2015 (Dataset S1). Pairs of images on the  
117 same orbit path, separated by either 6 or 12 days, are then co-registered using precise orbits.  
118 We use the SNAP offset tracking algorithm to produce initial velocity fields using a window  
119 of 128 x 128 pixels, before projecting it onto a WGS 84 grid at a pixel spacing of 300 m.  
120 Erroneous pixels were then removed if the difference from the MEaSURES velocity product  
121 was greater than  $\pm 50\%$ , before a 3x3 low pass filter was applied. Similarly high temporal  
122 resolution velocity time-series have been presented from Greenland using Sentinel-1 data  
123 (Lemos and others, 2018). We also use Sentinel-1 imagery to map changes in ice front  
124 position every 2 months between January 2014 and August 2018.

125

126 To produce a time-series of changes in ice speed between 2000 and 2017, we extracted mean  
127 ice speed from a  $\sim 50 \text{ km}^2$  box over the 2011 grounding line ('GL' on Fig. 1) obtained from  
128 the MEaSURES dataset (Rignot and others, 2011). In each epoch there were no missing  
129 pixels within the defined box. To produce further high temporal resolution time-series of ice  
130 speed between November 2013 and August 2018, and establish the spatial pattern of any  
131 change, we also extracted mean ice speed from three  $50 \text{ km}^2$  boxes further down-ice on the  
132 floating ice tongue (see Fig. 1). These include two locations in the shear zone between the  
133 Thwaites Glacier Tongue and its Eastern Ice Shelf (referred to as the Northern Shear Zone  
134 (NSZ) and the Southern Shear Zone (SSZ)) and on the Thwaites Eastern Ice Shelf (TEIS).  
135 Because the relative changes in the speed of the shear zone and Eastern Ice Shelf (at NSZ,

136 SSZ and TEIS) were much greater, we used the raw velocity fields i.e. without removing  
137 pixels greater than  $\pm 50\%$  of the MEaSURES dataset. To account for any bias arising from  
138 missing pixels, we only include time steps where at least 95% of pixels are present within  
139 each box.

140

141 To estimate the relative error (precision) in our high temporal resolution time-series of ice  
142 speed we first calculated the difference in ice speed between each successive point in the  
143 time-series at each location (e.g. TEIS, NSZ, SSZ and GL). The difference between each  
144 successive point represents the sum of the relative error and the trend or absolute change in  
145 speed between the two image pairs. To isolate the relative error we then subtracted the trend  
146 in ice speed change at each point, which we take as the moving average of the previous 10  
147 points in the time series. This produces median relative errors of  $\pm 0.22$ , 0.18, 0.17 and 0.07 m  
148  $\text{d}^{-1}$  ( $\pm 80$ , 66, 62 and 26  $\text{m yr}^{-1}$ ) for TEIS, NSZ, SSZ and GL, respectively. Some individual  
149 points have considerably higher relative errors, as reflected by the 90<sup>th</sup> percentiles of  $\pm 0.78$ ,  
150 0.59, 0.57 and 0.16  $\text{m d}^{-1}$  ( $\pm 284$ , 215, 208 and 58  $\text{m yr}^{-1}$ ), respectively. To account for these  
151 errors when comparing ice speeds at different time periods (e.g. difference between  
152 December 2015 and June 2018) we take a median of 10 consecutive velocity fields and  
153 assume a reasonable error to be the median relative error stated above.

154

155

### 156 **3. Results**

#### 157 **3.1 Annual observations (2000 – 2018)**

158

159 Our ice front data show that in 2000, Thwaites Glacier extended approximately 120 km  
160 seaward as an intact and coherent floating ice tongue (Fig. 2a). Since then, there have been  
161 significant changes to both its extent and structural integrity. Initially, in March 2002, the  
162 calving of a 3,400  $\text{km}^2$  tabular iceberg resulted in  $\sim 75$  km of ice-front retreat, before a re-  
163 advance occurred (Fig. 2a and 3a). Between 2006 and 2012 we observed the development of  
164 major rifting and fractures on the ice tongue around 20 and 35 km downstream of the  
165 grounding line and in the shear zone with the Thwaites Eastern Ice Shelf (Fig. 2b-e), but not  
166 further downstream near the ice-front. In 2012, another major tabular calving event resulted  
167 in the retreat of the ice-front 80 km behind its position in 2000 (see 2013 position on Fig. 2a  
168 and 3a). The 2012 calving event also marked the complete transition of the Thwaites Glacier  
169 Tongue from a largely intact ice tongue capable of the production of large tabular icebergs, to

170 a mélange of fractured icebergs ranging from around 1-5 km in width and bound together by  
171 sea-ice (Fig. 2f-j). The exception to this was at the ice-front, where a ~470 km<sup>2</sup> iceberg  
172 remained fastened to the ice front, a relic of the 2012 calving event (Fig. 2f, k). Until January  
173 2016, this iceberg was coalescent with the main Thwaites Tongue via dense ice mélange,  
174 which has known mechanical integrity (Rignot and MacAyeal, 1998). Between January and  
175 April 2016 it began to disintegrate.

176  
177 Overall, annual speed at the grounding line (averaged from box GL) increased ~38% between  
178 2000-2001 and 2016-2017 (from  $1,957 \pm 5$  m yr<sup>-1</sup> to  $2,696 \pm 32$  m yr<sup>-1</sup>). We note that there  
179 was little change in ice speed following the ~75 km retreat of its ice-front in 2002 (Fig. 3a,  
180 b). Most of the overall acceleration during the observation period took place between 2005-  
181 06 and 2011-12, where ice speed increased rapidly from  $2,072 \pm 32$  m yr<sup>-1</sup> to  $2,560 \pm 32$  m yr<sup>-1</sup>  
182 (Fig 3b). During this period of rapid acceleration there were no significant calving events and  
183 the ice-front steadily advanced (Fig. 3a). Thus, the period of rapid acceleration (Fig. 3b)  
184 coincides more generally with the onset of the structural weakening of the Thwaites Glacier  
185 Tongue between 2006 and 2012 (Fig. 2). From 2012-13 until 2015-16, there was a 6%  
186 slowdown in ice speed and the ice-front advanced (Fig. 3b). The largest annual increase in ice  
187 speed occurred between 2015-16 and 2016-17 where ice speed increased from  $2,530 \pm 32$  to  
188  $2,696 \pm 32$  m yr<sup>-1</sup> (Fig. 3b). Similar patterns in ice speed between 2000 and 2018 were present  
189 upstream of box GL, demonstrating that these changes in ice speed have not been caused by  
190 any ungrounding of ice in the vicinity of box GL, and are representative of wider changes in  
191 the system.

192

### 193 **3.2 High temporal resolution observations November 2013 – August 2018**

194

195 The high temporal resolution time series from Landsat-8 and Sentinel-1 (Fig. 4) shows  
196 substantial variability in glacier flow rates. Between November 2013 and December 2015 we  
197 observed a 9 km ice-front advance (Fig. 4e) and there was little change in ice speed at the  
198 grounding line; however, ice speed decreased along the eastern shear margin, by 22% in the  
199 northern shear zone (NSZ; Fig. 4b) and 10% in the southern shear zone (SSZ; Fig. 4c). In  
200 contrast, ice on the Thwaites Eastern Ice Shelf (TEIS; Fig. 4a) accelerated by 27% between  
201 November 2013 and December 2015. During this time period we observed no further  
202 structural weakening of the Ice Tongue and observed an advance of the structurally intact

203 boundary between the Thwaites Ice Tongue and the Eastern Ice Shelf (Fig. 5), indicating a  
204 strengthening of the shear margins.

205 There was a notable change in glacier behaviour in early 2016, when the velocity patterns  
206 across Thwaites Glacier switched: between January 2016 and March 2017, ice flow at the  
207 grounding line steadily accelerated by 7% (GL; Fig. 4d). This coincided with a rapid change  
208 in behaviour of ice in the eastern shear zone where, between January and May 2016, the  
209 northern shear zone accelerated by 75% (NSZ; Fig. 4b). Simultaneously, ice at the Thwaites  
210 Eastern Ice Shelf accelerated by 57% (TEIS; Fig. 4a) over the 5 month period. Whilst the  
211 near-instantaneous acceleration at the northern shear zone was maintained up to the end of  
212 the observational period, ice speed at the Thwaites Eastern Ice Shelf decreased by 60%  
213 between June 2016 and August 2018 (TEIS; 4a). This included a near-instantaneous decrease  
214 in ice speed of 40% between June 2016 and September 2016 (Fig. 4a). By August 2018, ice  
215 speed in the southern shear zone had increased by 68% (SSZ; Fig. 4c). The magnitude of this  
216 increase in ice speed is comparable to that of the NSZ, but unlike the abrupt increase there,  
217 the acceleration at the southern shear zone was more gradual (Fig. 4c). Coinciding with this  
218 speed-up, extensive rifts developed in the southern shear zone and, by October 2018, these  
219 had propagated to within a few kilometres of the grounding line (Fig. 5). Comparing the  
220 spatial pattern of velocity change both before (Nov 2013 – Dec 2015) and after (June 2016 –  
221 Aug 2018) January 2016, the largest velocity increase occurred along the eastern shear  
222 margin (Fig. 4f).

223 Between January 2016 and August 2018 the ice-front retreated by 16 km (Fig. 4e). This  
224 period coincides with the break-up of the large iceberg fastened to the ice-front between  
225 January 2016 and April 2016 (Fig. 6a). Notably, the break-up of this iceberg coincides with  
226 the onset of the acceleration across the ice tongue (Fig. 4b-c). A second large calving event  
227 took place in February 2017 (Fig. 6b) but, there were no coincident changes in velocity on the  
228 Thwaites Glacier Tongue.

229

#### 230 **4. Discussion**

231

232 As reported in previous studies (MacGregor and others, 2012), there was no significant  
233 change in the speed of Thwaites Glacier following the 75 km retreat of its ice-front as a result  
234 of the 2002 calving event (Fig. 3a, b), which confirms that the calved ice was ‘passive’ and

235 did not exert a significant buttressing effect (cf. Fürst and others, 2016). This lack of response  
236 in ice speed is consistent with theoretical explanations for an unconfined ice shelf  
237 (Sanderson, 1979). Indeed, longer-term observations show that there was no significant  
238 change in the speed of Thwaites Glacier between 1992 and 2005 (MacGregor and others,  
239 2012; Mouginot and others, 2014). However, ice speed increased by 24% between 2006 and  
240 2012, which coincides with the onset of the structural weakening and transition to *mélange* of  
241 the Thwaites Glacier Tongue and eastern shear zone (Fig. 2 and 3). Because shearing along  
242 the eastern margin of the Thwaites Glacier Tongue generates a stress that resists glacier flow  
243 (e.g. Rignot and others, 2006), any structural weakening of the ice tongue could create a  
244 positive feedback whereby structural weakening and accelerations reinforce each other (e.g.  
245 MacGregor and others, 2012). It has been hypothesized that this process could create a  
246 continuous process leading to further weakening of the shear margins until all resistance to  
247 ice shelf flow is lost (MacGregor and others, 2012).

248

249 Despite the major structural weakening and acceleration of Thwaites Glacier during the mid-  
250 2000s, it is clear that this has not been a continuous process. Between 2012 and 2015 ice  
251 speed on the main trunk of Thwaites Glacier decreased by 6% and there were no obvious  
252 signs of further structural weakening (Fig. 3 and 5). However, 2016 marks the beginning of  
253 another period of acceleration, structural weakening (Fig. 5), ice-front retreat (Fig. 4) and,  
254 indeed, grounding line retreat (Milillo and others, 2019). We now consider the extent to  
255 which these periods of structural weakening may have been triggered by an external forcing  
256 (Section 4.1), and we then examine the specific processes at play during the observed periods  
257 of change: the 2012-2015 slowdown (Section 4.2) and the 2016 acceleration (Section 4.3).  
258 We then explore the implications of the observed structural weakening on the interaction  
259 between the Thwaites Ice Tongue and landfast sea ice (Section 4.4).

260

#### 261 **4.1 Ocean temperature variability as a control on structural weakening of the Thwaites** 262 **Glacier Tongue**

263

264 Throughout the 20<sup>th</sup> and 21<sup>st</sup> centuries, oceanic conditions in the Amundsen Sea switched  
265 between periods of relative cool and extreme warmth (Jenkins and others, 2016; Jenkins and  
266 others, 2018). The onset of the structural weakening of the Thwaites Glacier Tongue  
267 coincided with a period of extremely warm oceanic conditions from the mid-2000s until the  
268 early 2010s, whilst the period of deceleration in the early 2010s coincides with cooler



269 conditions (Fig. 3c). This hints that ocean variability could be triggering the intermittent  
270 behaviour of Thwaites Glacier. Typically, such ocean variability is associated with changes at  
271 intermediate depth, at around 300-700 m (e.g. Jacobs and others, 2013; Dutrieux and others,  
272 2014; Jenkins and others, 2018), which is well below the ice tongue/mélange. However,  
273 increased melting in the vicinity of the grounding line could lead to the un-grounding of ice,  
274 reducing buttressing and subsequent acceleration of ice shelf flow, leading to a weakening of  
275 shear margins. Greater melting at depth and the associated shallower thermocline would also  
276 lead to more upwelling of warm water to the surface layers (Dutrieux and others, 2014),  
277 which could also directly weaken the ice shelf, mélange and shear margins, leading to further  
278 acceleration and ice-front retreat. A combination of both these processes could explain the  
279 link between ocean variability and the timing of the accelerations and structural weakening of  
280 Thwaites Glacier. In contrast, under relatively cool conditions, lower melt rates could slow  
281 down grounding line retreat and reduce melting of the ice tongue leading to a re-advance of  
282 the structurally intact shear margin boundary. In the following sections we discuss the  
283 importance of these physical mechanisms in the slowdown (2012-2015) and acceleration  
284 (2016-2018) of Thwaites Glacier using results from our high temporal resolution time series.

285

#### 286 **4.2 Slow-down of Thwaites Glacier between 2012 and 2015**

287

288 The slow-down of the main Thwaites Glacier Tongue between 2012 and 2015 could only be  
289 explained by a re-grounding of ice and thickening, or a strengthening of the shear margins.  
290 There is no reported evidence of the former (e.g. Milillo and others, 2019), but our results  
291 show that the margin between the Thwaites Glacier Tongue and the Thwaites Eastern Ice  
292 Shelf strengthened over this time period. Between November 2013 and December 2015 the  
293 boundary of structurally intact ice between the Thwaites Glacier Tongue and Eastern Ice  
294 Shelf advanced by 6 km (Fig. 5a-c), indicating a partial strengthening of the shear margin.  
295 Consistent with this strengthening is the reduction in velocity gradient between the faster  
296 flowing Thwaites Glacier Tongue and the slower flowing Thwaites Eastern Ice Shelf over the  
297 same time period (NSZ and TEIS; Fig 4a, b). Specifically, this is shown by a 22% reduction  
298 in ice speed at the faster flowing Thwaites Glacier Tongue (NSZ; Fig 4b) and a 27% increase  
299 in ice speed at the slower flowing Thwaites Eastern Ice Shelf (TEIS; Fig. 4a). This section of  
300 the Thwaites Eastern Ice Shelf (e.g. box TEIS) had been accelerating since 2008 (Mouginot  
301 and others, 2014), which was attributed to a partial ungrounding of a pinning point near the  
302 Thwaites Eastern Ice Shelf ice-front (Tinto and Bell, 2011; MacGregor and others, 2012) or

303 retreat of its grounding line (Rignot and others, 2014). Whilst these processes may be  
304 contributing to some of the longer-term acceleration, the pattern of velocity observed in our  
305 results (Fig. 4a, b) between November 2013 and December 2015 is entirely consistent with a  
306 partial recoupling in flow between the Thwaites Glacier Tongue and Eastern Ice Shelf  
307 between November 2013 and December 2015. This is where the faster flowing and more  
308 dominant Thwaites Glacier Tongue entrains the slower Thwaites Eastern Ice Shelf, resulting  
309 in its acceleration. Simultaneously, the greater shear stresses associated with a stronger shear  
310 margin results in a slowdown in velocity of the Thwaites Glacier Tongue.

311

312 Whilst our results suggest the strengthening of shear margins are likely to have been  
313 important in the slowdown of the Thwaites Glacier, other factors may also have contributed  
314 to the slowdown. One possibility is that the ice tongue may have re-grounded onto a pinning  
315 point or increased in grounded area. Based on the 2011 grounding line (Rignot and others  
316 2011), the ice tongue was likely stabilised by at least three small pinning points (Fig. 1). It is  
317 possible that small changes in ice tongue thickness could have increased the grounded area  
318 and contributed to the slowdown. However, this is difficult to assess because no additional  
319 grounding line observations are available over this time period.

320

### 321 **4.3 January 2016 acceleration**

322

323 January 2016 marks the onset of a period of acceleration across the grounding line,  
324 weakening of the shear margins and a retreat of both the grounding line (e.g. Milillo and  
325 others, 2019) and ice-front. The most rapid changes in ice speed occurred at the NSZ and at  
326 the TEIS, where in January 2016 ice speed increased by 75% and 57%, respectively, over the  
327 course of a few weeks (Fig. 4a, b). This resulted in a rapid steepening of the velocity gradient  
328 between the Thwaites Glacier Tongue and the TEIS, which ultimately led to further structural  
329 damage and a decoupling in flow between the two ice shelves. Consistent with this is the  
330 rapid 60% deceleration of TEIS from August 2017 to February 2018 (Fig. 4a), associated  
331 with a reduction in shear from the faster flowing ice tongue. This pattern of velocity change  
332 is very similar to that reported by Mouginot and others (2014) at the onset of Thwaites  
333 Glacier's last major acceleration event in 2006. Thus, following the reported decoupling in  
334 flow between the two ice shelves in 2006, ice flow has since partially recoupled between  
335 2013 and 2015, before decoupling again in 2016.

336

337 The acceleration of ice in the SSZ (Fig. 4c) in January 2016 was at a comparatively slower  
338 rate than ice in the NSZ (Fig. 4b), creating a steep velocity gradient. Over the following  
339 months, the increased longitudinal stresses associated with the steep velocity gradient (e.g.  
340 Benn and others, 2007) resulted in the development of a series of rifts along the eastern shear  
341 zone and to within a few kilometres of the grounding line (Fig. 5). The loss of buttressing  
342 associated with the weakening of the shear zone, may have played an important role in the  
343 increase in ice speed observed at the grounding line (e.g. Fig. 4d). Consistent with this is the  
344 spatial pattern of velocity change, which indicates that the largest increases in velocity are  
345 concentrated along the entire eastern margin (Fig. 4f).

346

347 The mechanism responsible for the initial increase in ice speed towards the ice-front at the  
348 NSZ (Fig. 4b), in January 2016, is unclear. One possibility is that the rapid increase in speed  
349 at NSZ was a direct consequence of the break-up and calving of the large structurally intact  
350 iceberg fastened to the ice-front (Fig. 6a). This iceberg may have been acting as an obstacle,  
351 helping to pin the mélange in the shear zone, meaning the break-up of the iceberg resulted in  
352 a near-instantaneous loss of buttressing in the northern shear zone. Consistent with this is the  
353 near-instantaneous acceleration of ice at NSZ (Fig. 4b), which observations elsewhere have  
354 shown to be a typical response to calving events which reduce buttressing (e.g. Scambos and  
355 others, 2004). In addition, the mélange at in the northern shear zone may have been weakened  
356 through a combination of enhanced ocean melt, the seasonal retreat of landfast sea-ice, and  
357 by surface melt. Indeed, it is notable that in January 2016 an anomalously large amount of  
358 surface melt was produced in the Thwaites embayment (Nicolas and others, 2017). An  
359 alternative explanation is that the acceleration at the NSZ could be linked to a rapid  
360 grounding line retreat which occurred over a similar time period to the observed acceleration  
361 (Milillo and others, 2019), or un-grounding of any pinning points. However, this seems  
362 unlikely because the acceleration of the northern shear zone occurred before any large  
363 increases in speed upstream either at the southern shear zone or at the grounding line (Fig.  
364 4a-d), which would be expected if grounding line retreat was the driver. Rather, after the  
365 initial weakening of the shear margins, grounding line retreat may have accelerated the inland  
366 propagation of structural weakening of the eastern shear margin. Regardless of the physical  
367 mechanism responsible for the initial increase in ice speed at NSZ, our results show that  
368 despite extensive structural weakening of the Thwaites Glacier Tongue, processes originating  
369 in the shear zone towards the ice-front between the Thwaites Glacier Tongue and Eastern Ice  
370 shelf are still playing an important role in ice dynamics towards the grounding line. This

371 highlights the importance in understanding the mechanisms which may lead to future changes  
372 in the stability of the ice tongue in the future.

373

#### 374 **4.4 Interaction between the Thwaites Ice Tongue and landfast sea ice**

375

376 The overall structural weakening of the Thwaites Glacier Tongue over the past two decades is  
377 likely to render it far more vulnerable to further retreat or disintegration in the near-future.  
378 For example, its present-day structure now strongly resembles Holmes Glacier in Porpoise  
379 Bay, (Fig. 7a, b) which is reliant on multi-year landfast sea-ice for structural integrity, and  
380 where sea-ice break-out events have been shown to trigger disintegration of large sections of  
381 its floating ice tongue (Fig. 7a; Miles and others, 2017). Elsewhere, the mechanical binding  
382 of landfast sea ice to the Mertz Glacier tongue has been shown to be important for the ice  
383 tongue's integrity (Massom and others, 2015). Given that the western margin of the Thwaites  
384 Glacier Tongue is also fastened to a band of multi-year sea-ice, we hypothesize that the  
385 recently weakened Thwaites Glacier Tongue may now also have some dependency on  
386 landfast sea-ice for structural integrity. The implication is that future break-outs of multi-year  
387 sea-ice in front of the Thwaites Glacier Tongue could result in further structural weakening or  
388 even disintegration. This is supported by observations of the initiation of a partial break-out  
389 of multi-year sea-ice in February 2019, which has resulted in the disintegration of a small  
390 section of the Thwaites Glacier Tongue on the western margin (Fig. 7b). Taken together, this  
391 means that the Thwaites Glacier Tongue would become more vulnerable to disintegration if  
392 landfast sea-ice or pack-ice were to become less persistent in the future.

393

394 Landfast sea-ice is sensitive to changes in the ocean-climate system (Mahoney and others,  
395 2007; Fraser and others, 2012). Individual break-out events can be driven by extreme climatic  
396 events (Fraser and others, 2012; Aoki and others, 2017; Miles and others, 2017), but abrupt  
397 changes can be also be caused by changes in the local ice-scape (e.g. Tamura and others,  
398 2012; Massom and others, 2013; Campagne and others, 2015). An important component of  
399 the local sea-ice regime in the Thwaites embayment is the grounded B-22a iceberg (e.g.  
400 Stammerjohn and others 2015), which lies ~130 km out to sea north-east of Thwaites Glacier  
401 (Fig. 7c). Several studies have highlighted the importance of grounded icebergs or ice  
402 tongues (e.g. Mertz) acting as 'anchors', which help to facilitate growth and stabilize landfast  
403 sea-ice regimes (e.g. Fraser and others, 2012; Massom and others, 2010; 2013; Stammerjohn  
404 and others, 2015). Notably, the band of multi-year landfast sea-ice attached to the western

405 margin of the Thwaites Glacier Tongue is also anchored to the B-22a iceberg, suggesting that  
406 the iceberg is likely aiding the stability of the landfast sea-ice (Fig. 7c). Therefore, when the  
407 grounded iceberg is removed from the Thwaites embayment (likely in the near-future), a  
408 change to less favourable landfast sea-ice conditions is likely to occur. Any decrease in  
409 landfast sea-ice persistency or extent would ultimately increase the prospect of further retreat  
410 or disintegration of the Thwaites Ice Tongue. This is important because whilst the tongue  
411 may only be providing a small amount of buttressing through its interaction with the Eastern  
412 Ice Shelf, it still acts as an important buffer for the inner ice shelf, by limiting potential  
413 damage from ocean waves and swell (e.g. Massom and others, 2018). Moreover, changes in  
414 either the ice tongue or landfast sea-ice extent could also have important implications on  
415 regional ocean circulation, with potential implications for melt rates at the grounding line  
416 (e.g. Webber and others, 2017).

417

418

## 419 **5. Summary**

420

421 Over the last 18 years, Thwaites Glacier Tongue has retreated >80 km, accelerated by 38%,  
422 and has transitioned from a structurally-intact ice tongue capable of producing large tabular  
423 icebergs, to a mélange of smaller fractured icebergs bounded by sea-ice. However, the rate of  
424 change throughout the observational period has not been uniform and we identify two distinct  
425 acceleration phases, separated by a period of deceleration. The largest acceleration took place  
426 between 2006 and 2012 when there was extensive structural weakening of the ice tongue and  
427 shear margins, along with a 23% increase in ice speed. However, between 2012 and 2015  
428 there was a 6% slowdown in ice flow on the main Thwaites Glacier trunk, and there was a  
429 partial recoupling in flow between the Thwaites Glacier Tongue and the Eastern Ice Shelf as  
430 the structurally intact shear margin boundary advanced. The most recent acceleration started  
431 in January 2016 and is characterised by a major weakening of the eastern shear margin,  
432 which initiated on the ice tongue and, over the following months, propagated towards the  
433 grounding line as velocity gradients increased. The timing of the first acceleration coincides  
434 with a period of relatively warm ocean conditions, whilst relatively cool ocean conditions  
435 coincide with the deceleration phase. This correlation suggests that the ocean may be acting  
436 as trigger for these distinct episodes of glacier behaviour.

437 Despite the major structural weakening of the Thwaites Glacier Tongue it may still be  
438 playing an import role in ice dynamics at the grounding line, meaning future changes in its  
439 extent are still an important consideration. As a result of the structural weakening over the  
440 past 18 years the Thwaites Ice Tongue now has some dependency on landfast sea-ice for  
441 structural integrity. The removal of iceberg B-22a from the Thwaites embayment could result  
442 in a regime change, in that a reduction in the persistency of landfast sea-ice would have  
443 detrimental impacts on the ice tongue's future structural integrity. There is a need for these  
444 complex processes associated with weakening ice tongues to be explored quantitatively  
445 through numerical modelling because they may have important implications for the rates of  
446 future sea level contributions.

447

448

449 **Acknowledgements** This work was funded by the Natural Environment Research Council  
450 (grant number: NE/R000824/1). MODIS imagery from the NASA WorldView Explorer is  
451 available at <https://worldview.earthdata.nasa.gov/>. Sentinel-1 imagery is available from the  
452 Copernicus Open Access Hub (<https://scihub.copernicus.eu/>). Landsat imagery is freely  
453 available and can be downloaded via Earth Explorer (<https://earthexplorer.usgs.gov/>). ESA  
454 SNAP software can be freely downloaded at <http://step.esa.int/main/download/>. GoLive  
455 Landsat-8 velocities are available at <https://doi.org/10.7265/N5ZP442B>. Amundsen Sea  
456 velocities from 2000 and 2002 are available at  
457 <https://doi.org/10.5067/MEASURES/CRYOSPHERE/nsidc-0545.001>. MEaSURES annual  
458 ice velocity maps are available at <https://doi.org/10.5067/9T4EPQXTJYW9>. Grounding lines  
459 data are available at <https://doi.org/10.5067/IKBWW4RYHF1Q>. Ice-front positions collected  
460 in this study will be deposited in the NERC polar observation data centre upon publication.  
461 Velocity time series are available as a supplementary dataset. We would like to thank two  
462 anonymous reviewers and the editor – Helen Amanda Fricker - for providing constructive  
463 comments which led to the improvement of this manuscript.

464

465

466

467

468 **References**

- 469 Aoki, S. (2017), Breakup of land-fast sea ice in Lutzow-Holm Bay, East Antarctica, and its  
470 teleconnection to tropical Pacific sea surface temperatures, *Geophys Res Lett*, 44(7), 3219-3227.
- 471 Benn, D. I., C. R. Warren, and R. H. Mottram (2007), Calving processes and the dynamics of calving  
472 glaciers, *Earth-Science Reviews*, 82(3-4), 143-179.
- 473 Campagne, P., and others (2015), Glacial ice and atmospheric forcing on the Mertz Glacier Polynya  
474 over the past 250 years, *Nat Commun*, 6.
- 475 DeConto, R. M., and D. Pollard (2016), Contribution of Antarctica to past and future sea-level rise,  
476 *Nature*, 531(7596), 591-+.
- 477 Dutrieux, P., J. De Rydt, A. Jenkins, P. R. Holland, H. K. Ha, S. H. Lee, E. J. Steig, Q. H. Ding, E. P.  
478 Abrahamsen, and M. Schroder (2014), Strong Sensitivity of Pine Island Ice-Shelf Melting to Climatic  
479 Variability, *Science*, 343(6167), 174-178.
- 480 Edwards, T.L., Brandon, M.A., Durand, G. et al. (2019) Revisiting Antarctic ice loss due to marine  
481 ice-cliff instability. *Nature* 566, 58–64.
- 482 Fahnestock, M., T. Scambos, T. Moon, A. Gardner, T. Haran, and M. Klinger (2016), Rapid large-  
483 area mapping of ice flow using Landsat 8, *Remote Sens Environ*, 185, 84-94.
- 484 Fraser, A. D., R. A. Massom, K. J. Michael, B. K. Galton-Fenzi, and J. L. Lieser (2012), East  
485 Antarctic Landfast Sea Ice Distribution and Variability, 2000-08, *J Climate*, 25(4), 1137-1156.
- 486 Fretwell, P., and others (2013), Bedmap2: improved ice bed, surface and thickness datasets for  
487 Antarctica, *Cryosphere*, 7(1), 375-393.
- 488 Furst, J. J., Durand, G., Gillet-Chaulet, F., Tavard, L., Rankl, M., Braun, M., and Gagliardini, O.  
489 (2016): The safety band of Antarctic ice shelves, *Nat. Clim. Change*, 6, 479–482.
- 490 Gollede, N. R., D. E. Kowalewski, T. R. Naish, R. H. Levy, C. J. Fogwill, and E. G. W. Gasson  
491 (2015), The multi-millennial Antarctic commitment to future sea-level rise, *Nature*, 526(7573), 421-+.
- 492 Gudmundsson, G. H., Krug, J., Durand, G., Favier, L. and Gagliardini, O. (2012): The stability of  
493 grounding lines on retrograde slopes, *Cryosphere*, 6(6), 1497–1505, doi:10.5194/tc-6-1497-2012.
- 494 Gudmundsson, G. H. (2013), Ice-shelf buttressing and the stability of marine ice sheets, *Cryosphere*,  
495 7(2), 647–655, doi:10.5194/tc-7-647-2013.

496 Gudmundsson, G. H., Paolo, F. S., Adusumilli, S., & Fricker, H. A. ( 2019). Instantaneous Antarctic  
497 ice- sheet mass loss driven by thinning ice shelves. *Geophysical Research Letters*, 46, 13903– 13909.

498 Holt, J. W., Blankenship, D. D., Morse, D. L., Young, D. A., Peters, M. E., Kempf, S. D., Richter, T.  
499 G., Vaughan, D. G., and Corr, H. F. J. ( 2006), New boundary conditions for the West Antarctic Ice  
500 Sheet: Subglacial topography of the Thwaites and Smith glacier catchments, *Geophys. Res. Lett.*, 33,  
501 L09502, doi:[10.1029/2005GL025561](https://doi.org/10.1029/2005GL025561).

502 Jacobs, S., C. Giulivi, P. Dutrieux, E. Rignot, F. Nitsche, and J. Mouginot (2013), Getz Ice Shelf  
503 melting response to changes in ocean forcing, *Journal of Geophysical Research: Oceans*, 118(9),  
504 4152-4168.

505 Jenkins, A., P. Dutrieux, S. S. Jacobs, S. D. McPhail, J. R. Perrett, A. T. Webb, and D. White (2010),  
506 Observations beneath Pine Island Glacier in West Antarctica and implications for its retreat, *Nat*  
507 *Geosci*, 3(7), 468-472.

508 Jenkins, A., P. Dutrieux, S. Jacobs, E.J. Steig, G.H. Gudmundsson, J. Smith, and K.J. Heywood.  
509 (2016), Decadal ocean forcing and Antarctic ice sheet response: Lessons from the Amundsen Sea.  
510 *Oceanography* 29(4):106–117, <https://doi.org/10.5670/oceanog.2016.103>.

511 Jenkins, A., D. Shoosmith, P. Dutrieux, S. Jacobs, T. W. Kim, S. H. Lee, H. K. Ha, and S.  
512 Stammerjohn (2018), West Antarctic Ice Sheet retreat in the Amundsen Sea driven by decadal oceanic  
513 variability, *Nat Geosci*, 11(10), 733-+.

514 Joughin, I., B. E. Smith, and B. Medley (2014), Marine Ice Sheet Collapse Potentially Under Way for  
515 the Thwaites Glacier Basin, West Antarctica, *Science*, 344(6185), 735-738.

516 Konrad, H., A. Shepherd, L. Gilbert, A. E. Hogg, M. McMillan, A. Muir, and T. Slater (2018), Net  
517 retreat of Antarctic glacier grounding lines, *Nat Geosci*, 11(4), 258-+.

518 Lemos, A., A. Shepherd, M. McMillan, A. E. Hogg, E. Hatton, and I. Joughin (2018), Ice velocity of  
519 Jakobshavn Isbr ae, Petermann Glacier, Nioghalvfjærdsfjorden, and Zacharias Isstrom, 2015-2017,  
520 from Sentinel 1-a/b SAR imagery, *Cryosphere*, 12(6), 2087-2097.

521 MacGregor, J. A., G. A. Catania, M. S. Markowski, and A. G. Andrews (2012), Widespread rifting  
522 and retreat of ice-shelf margins in the eastern Amundsen Sea Embayment between 1972 and 2011, *J*  
523 *Glaciol*, 58(209), 458-466.

524 Mahoney, A., H. Eicken, A. G. Gaylord, and L. Shapiro (2007), Alaska landfast sea ice: Links with  
525 bathymetry and atmospheric circulation, *J Geophys Res-Oceans*, 112(C2).



526 Massom, R., P. Reid, S. Stammerjohn, B. Raymond, A. Fraser, and S. Ushio (2013), Change and  
527 Variability in East Antarctic Sea Ice Seasonality, 1979/80-2009/10, *Plos One*, 8(5).

528 Massom, R. A., Giles, A. B., Warner, R. C., Fricker, H. A., Legrésy, B., Hyland, G., Lescarmonier,  
529 L., and Young, N. (2015), External influences on the Mertz Glacier Tongue (East Antarctica) in the  
530 decade leading up to its calving in 2010. *J. Geophys. Res. Earth Surf.*, 120, 490– 506.

531 Massom, R. A., T. A. Scambos, L. G. Bennetts, P. Reid, V. A. Squire, and S. E. Stammerjohn (2018),  
532 Antarctic ice shelf disintegration triggered by sea ice loss and ocean swell, *Nature*, 558(7710), 383-+.

533 McMillan, M., A. Shepherd, A. Sundal, K. Briggs, A. Muir, A. Ridout, A. Hogg, and D. Wingham  
534 (2014), Increased ice losses from Antarctica detected by CryoSat-2, *Geophys Res Lett*, 41(11), 3899-  
535 3905.

536 Mercer, J. H. (1978), West Antarctic Ice Sheet and Co2 Greenhouse Effect - Threat of Disaster,  
537 *Nature*, 271(5643), 321-325.

538 Miles, B. W. J., C. R. Stokes, and S. S. R. Jamieson (2016), Pan-ice-sheet glacier terminus change in  
539 East Antarctica reveals sensitivity of Wilkes Land to sea-ice changes, *Science Advances*, 2(5).

540 Miles, B. W. J., C. R. Stokes, and S. S. R. Jamieson (2017), Simultaneous disintegration of outlet  
541 glaciers in Porpoise Bay (Wilkes Land), East Antarctica, driven by sea ice break-up, *The Cryosphere*,  
542 11(1), 427-442.

543 Milillo, P., E. Rignot, P. Rizzoli, B. Scheuchl, J. Mouginot, J. Bueso-Bello, and P. Prats-Iraola (2019),  
544 Heterogeneous retreat and ice melt of Thwaites Glacier, West Antarctica, *Science Advances*, 5(1).

545 Millan, R., E. Rignot, V. Bernier, M. Morlighem, and P. Dutrieux (2017), Bathymetry of the  
546 Amundsen Sea Embayment sector of West Antarctica from Operation IceBridge gravity and other  
547 data, *Geophys Res Lett*, 44(3), 1360-1368.

548 Moon, T., and I. Joughin (2008), Changes in ice front position on Greenland's outlet glaciers from  
549 1992 to 2007, *J Geophys Res-Earth*, 113(F2).

550 Mouginot, J., E. Rignot, and B. Scheuchl (2014), Sustained increase in ice discharge from the  
551 Amundsen Sea Embayment, West Antarctica, from 1973 to 2013, *Geophys Res Lett*, 41(5), 1576-  
552 1584.

553 Mouginot, J., E. Rignot, B. Scheuchl, and R. Millan (2017), Comprehensive Annual Ice Sheet  
554 Velocity Mapping Using Landsat-8, Sentinel-1, and RADARSAT-2 Data, *Remote Sens-Basel*, 9(4).

555 Nicolas, J. P., and others (2017), January 2016 extensive summer melt in West Antarctica favoured by  
556 strong El Niño, *Nature Communications*, 8, 15799.

557 Paolo, F. S., H. A. Fricker, and L. Padman (2015), Volume loss from Antarctic ice shelves is  
558 accelerating, *Science*, 348(6232), 327-331.

559 Pollard, D., R. M. DeConto, and R. B. Alley (2015), Potential Antarctic Ice Sheet retreat driven by  
560 hydrofracturing and ice cliff failure, *Earth Planet Sc Lett*, 412, 112-121.

561 Rignot, E., & MacAyeal, D. (1998). Ice-shelf dynamics near the front of the Filchner—Ronne Ice  
562 Shelf, Antarctica, revealed by SAR interferometry. *Journal of Glaciology*, 44(147), 405-418.

563 Rignot, E., J. Mouginot, and B. Scheuchl (2011), Antarctic grounding line mapping from differential  
564 satellite radar interferometry, *Geophys Res Lett*, 38.

565 Rignot, E. (2006), Changes in ice dynamics and mass balance of the Antarctic ice sheet, *Philosophical*  
566 *Transactions of the Royal Society a-Mathematical Physical and Engineering Sciences*, 364(1844),  
567 1637-1655.

568 Rignot, E., J. Mouginot, and B. Scheuchl (2011), Ice Flow of the Antarctic Ice Sheet, *Science*,  
569 333(6048), 1427-1430.

570 Rignot, E., Mouginot, J., Morlighem, M., Seroussi, H., and Scheuchl, B. ( 2014), Widespread, rapid  
571 grounding line retreat of Pine Island, Thwaites, Smith, and Kohler glaciers, West Antarctica, from  
572 1992 to 2011, *Geophys. Res. Lett.*, 41, 3502– 3509

573 Rignot, E., J. Mouginot, B. Scheuchl, M. van den Broeke, M. J. van Wessem, and M. Morlighem  
574 (2019), Four decades of Antarctic Ice Sheet mass balance from 1979–2017, *Proceedings of the*  
575 *National Academy of Sciences*, 116(4), 1095-1103.

576 Sanderson, T. (1979). Equilibrium Profile of Ice Shelves. *Journal of Glaciology*, 22(88), 435-460.  
577 doi:10.3189/S0022143000014453

578 Scambos, T. A., J. A. Bohlander, C. A. Shuman, and P. Skvarca (2004), Glacier acceleration and  
579 thinning after ice shelf collapse in the Larsen B embayment, Antarctica, *Geophysical Research*  
580 *Letters*, 31(18).

581 Scambos, T. A., and others (2017), How much, how fast?: A science review and outlook for research  
582 on the instability of Antarctica's Thwaites Glacier in the 21st century, *Global Planet Change*, 153, 16-  
583 34.

584 Schoof, C. (2007), Ice sheet grounding line dynamics: Steady states, stability, and hysteresis, *J*  
585 *Geophys Res-Earth*, 112(F3).

586 Seroussi, H., Y. Nakayama, E. Larour, D. Menemenlis, M. Morlighem, E. Rignot, and A. Khazendar  
587 (2017), Continued retreat of Thwaites Glacier, West Antarctica, controlled by bed topography and  
588 ocean circulation, *Geophys Res Lett*, 44(12), 6191-6199.

589 Shepherd, A., and others (2018), Mass balance of the Antarctic Ice Sheet from 1992 to 2017, *Nature*,  
590 558(7709), 219-+.

591 Stammerjohn, S.E., Maksym, T., Massom, R.A., Lowry, K.E., Arrigo, K.R., Yuan, X., Raphael, M.,  
592 Randall-Goodwin, E., Sherrell, R.M. and Yager, P.L., (2015), Seasonal sea ice changes in the  
593 Amundsen Sea, Antarctica, over the period of 1979–2014. *Elem Sci Anth*, 3.

594 Tamura, T., G. D. Williams, A. D. Fraser, and K. I. Ohshima (2012), Potential regime shift in  
595 decreased sea ice production after the Mertz Glacier calving, *Nat Commun*, 3.

596 Tinto, K. J., and R. E. Bell (2011), Progressive unpinning of Thwaites Glacier from newly identified  
597 offshore ridge: Constraints from aerogravity, *Geophys Res Lett*, 38.

598 Thoma, M., A. Jenkins, D. Holland, and S. Jacobs (2008), Modelling Circumpolar Deep Water  
599 intrusions on the Amundsen Sea continental shelf, Antarctica, *Geophys Res Lett*, 35(18).

600 Webber, B. G. M., K. J. Heywood, D. P. Stevens, P. Dutrieux, E. P. Abrahamsen, A. Jenkins, S. S.  
601 Jacobs, H. K. Ha, S. H. Lee, and T. W. Kim (2017), Mechanisms driving variability in the ocean  
602 forcing of Pine Island Glacier, *Nat Commun*, 8.

603

604

605

606

607

608

609

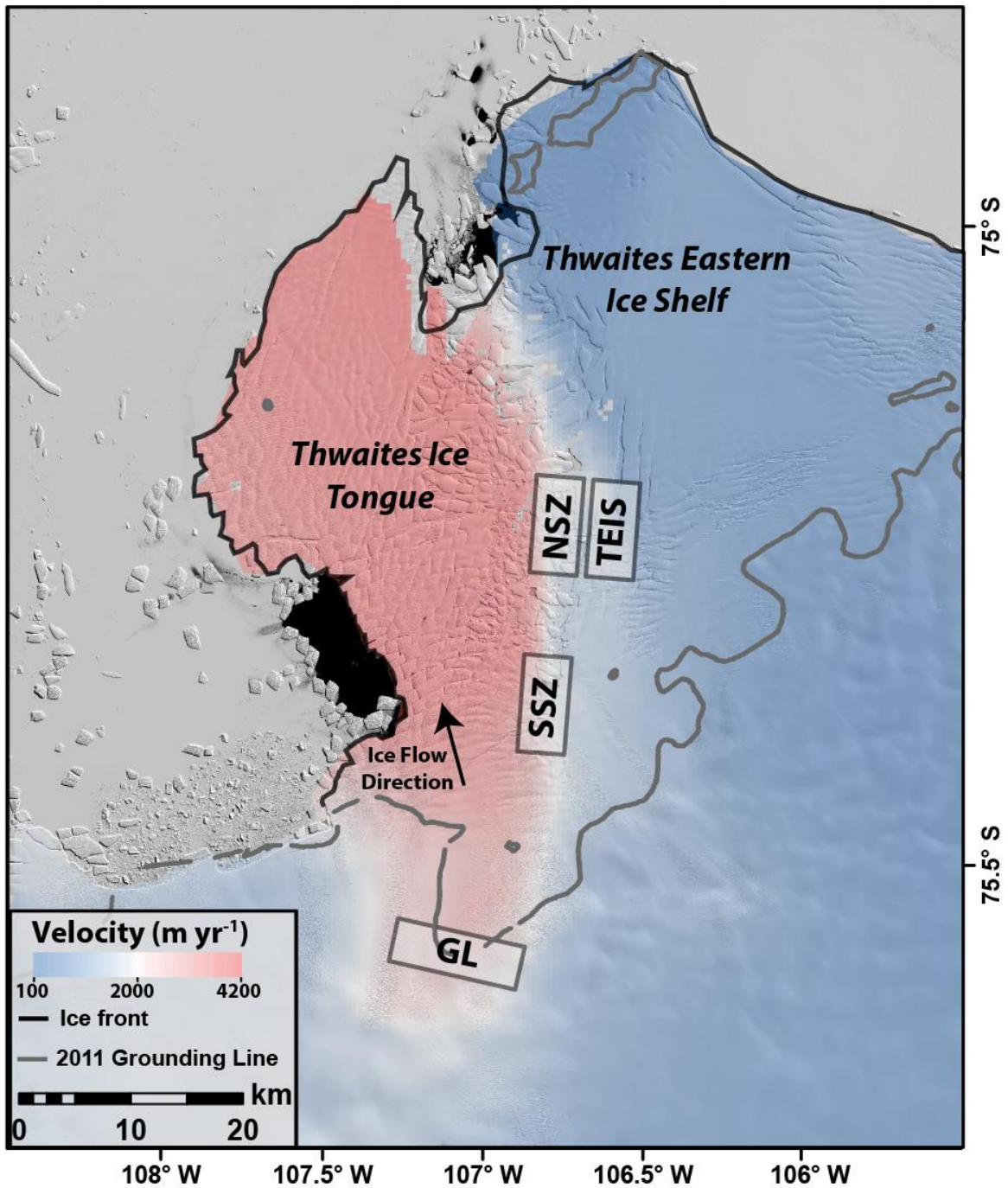
610

611

612

613

614

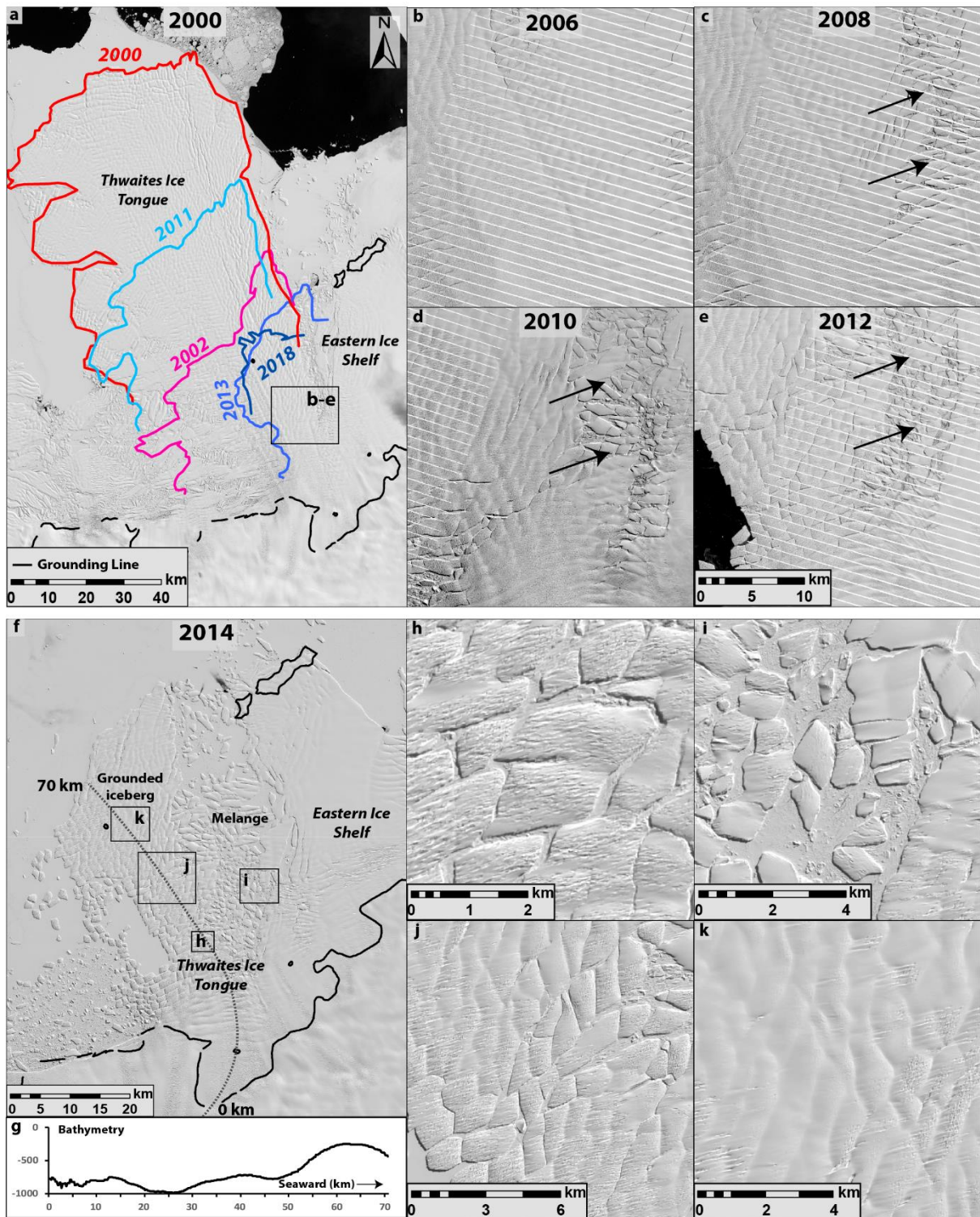


616

617 **Figure 1:** Landsat-8 image from November 2013 of the Thwaites Ice Tongue and Eastern Ice  
 618 Shelf, overlain with the MEaSUREs 2011 grounding line (Rignot and others, 2011) and the  
 619 MEaSUREs composite velocity product. The boxes where our velocity time series are  
 620 extracted as spatial averages: Northern Shear Zone (NSZ), Southern Shear Zone (SSZ),  
 621 Thwaites Eastern Ice Shelf (TEIS) and Grounding Line (GL). Note the steep velocity gradient  
 622 between the Thwaites Ice Tongue and Eastern Ice Shelf.

623



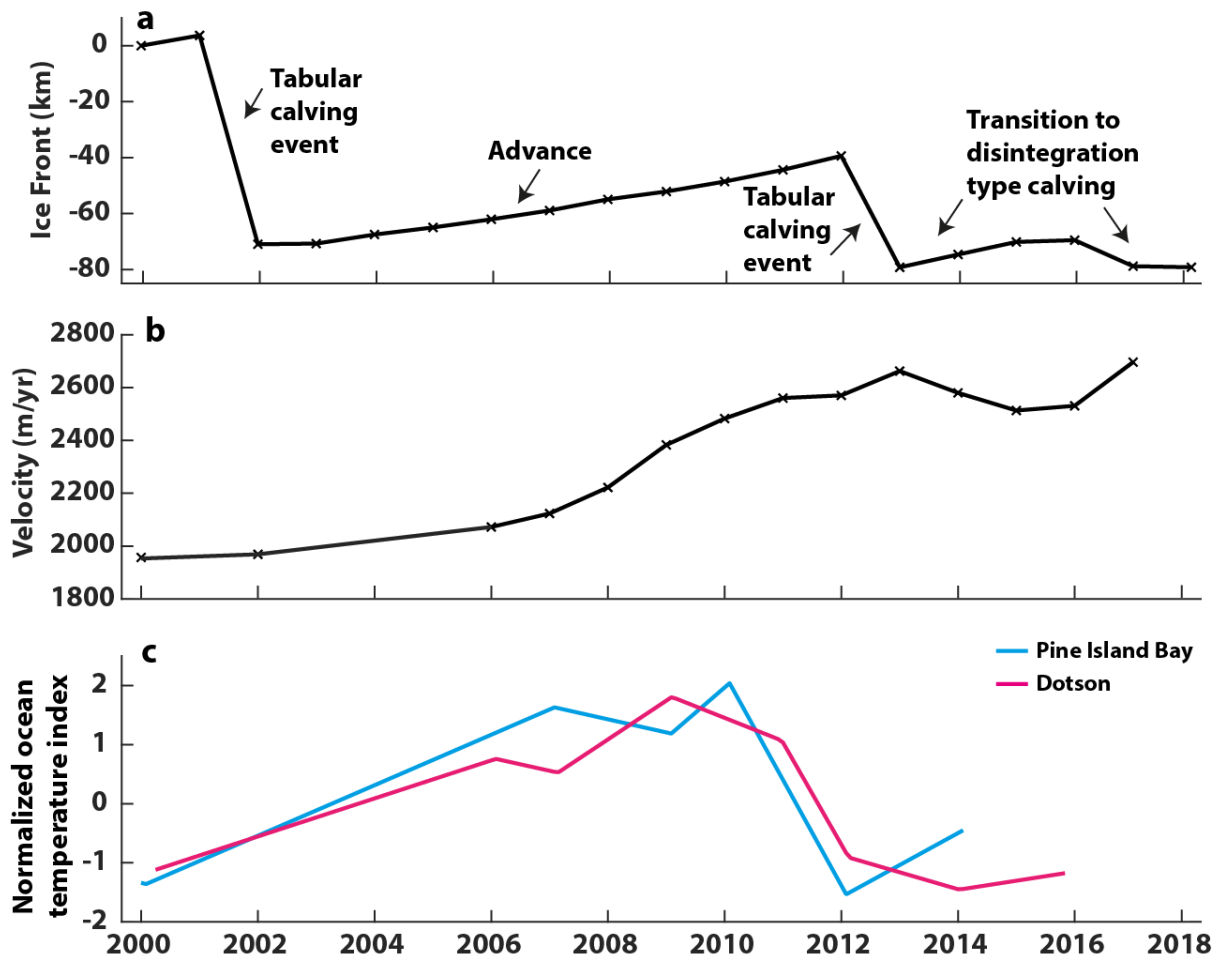


624

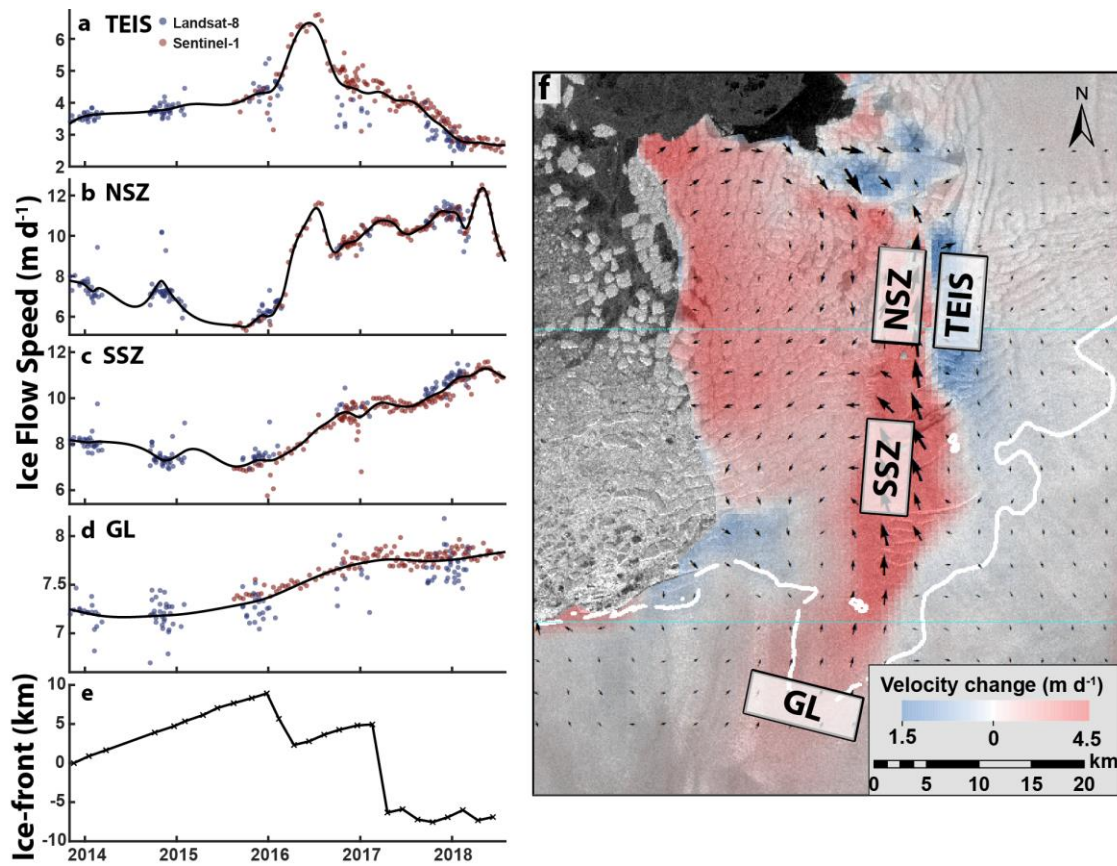
625

626 **Figure 2:** Structural transition of the Thwaites Glacier Tongue. **a)** Landsat-7 image of the  
 627 120 km long Thwaites Glacier Tongue in 2000 with digitized ice-front positions. The  
 628 grounding line is from the MEaSUREs dataset in 2011 (Rignot and others, 2011). **b-e)**  
 629 Landsat-7 images showing the changes in structure of the Thwaites Glacier Tongue. The  
 630 black arrows point to the development of rifts in each successive image. The location of these

631 images is shown by the black boxes in 1a. **f)** Landsat-8 image in 2014 weakened ice tongue.  
 632 Note the structurally intact grounded iceberg. **g)** Bathymetry (Millan and others, 2017) taken  
 633 along the transect shown in 1f (dotted line). Note the presence of the offshore ridge. **h-k)**  
 634 Close-ups of the Thwaites Glacier Tongue from 2014, the location of each image is shown in  
 635 black boxes in f.  
 636  
 637



638  
 639  
 640 **Figure 3:** Annual ice-front (a) and velocity (b) changes 2000 and 2018. c) Normalized ocean  
 641 temperature index from Pine Island Bay (blue line; Jenkins and others, 2016) and Dotson  
 642 (cyan line; Jenkins and others, 2018). Note the switch to cooler conditions in 2012.

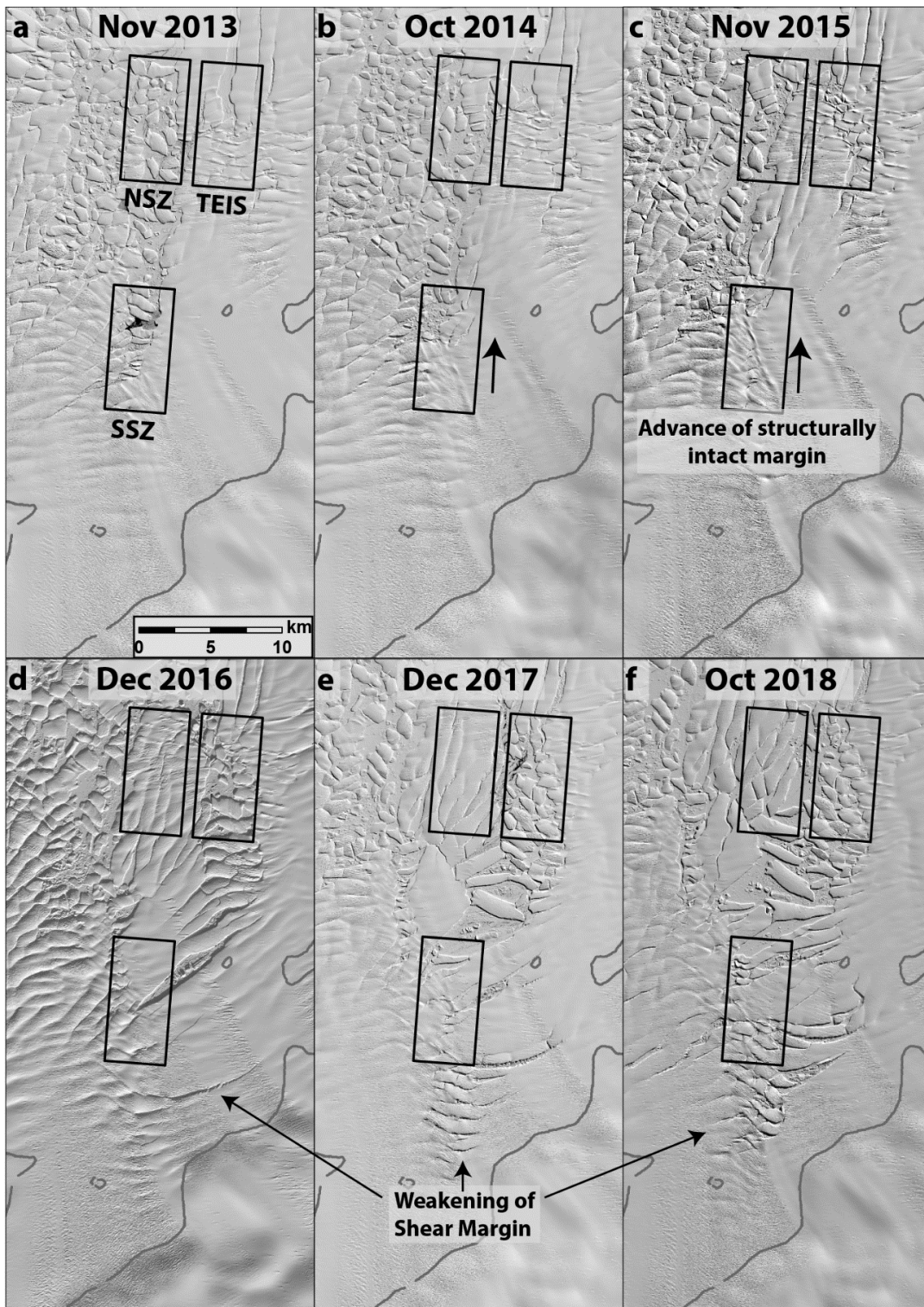


643

644

645 **Figure 4:** High temporal resolution ice speed and ice-front position changes between  
 646 November 2013 and August 2018. a) Thwaites Eastern Ice Shelf (TEIS) b) Northern Shear  
 647 Zone (NSZ) c) Southern Shear Zone (SSZ) d) Grounding Line (GL). The black line in each  
 648 velocity panel is a smoothing spline. e) Changes in ice-front position. f) Difference in median  
 649 velocity before January 2016 (Nov 2013-Dec 2015) and after (June 2016 – Aug 2018)  
 650 overlain on a Sentinel-1 image from August 2018, with red indicating a velocity increase and  
 651 blue a decrease. Note the largest increases in velocity occur in the eastern shear zone.

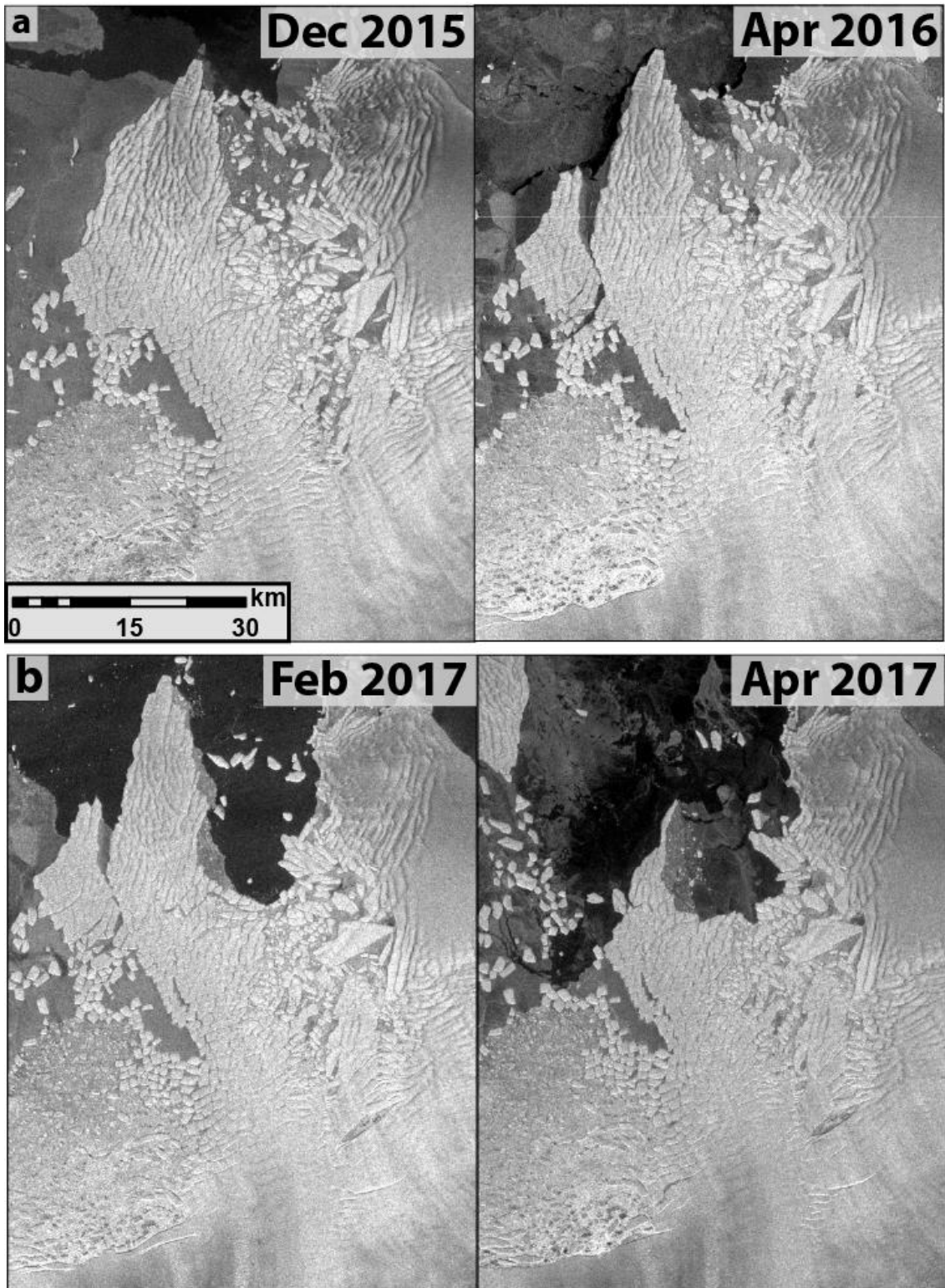




652

653 **Figure 5:** Landsat 8 images from 2013 to 2018 showing the structural changes at the shear  
 654 margin between the Thwaites Ice Tongue and Eastern Ice Shelf. From 2013 to 2015 (a-c),  
 655 there are no signs of further structural weakening and the structurally intact boundary  
 656 between the ice tongue and Eastern Ice Shelf advances. From 2016 to 2018 (d-f) there is  
 657 extensive structural weakening of the shear margin. The grey line is the 2011 grounding line  
 658 (Rignot and others, 2011).



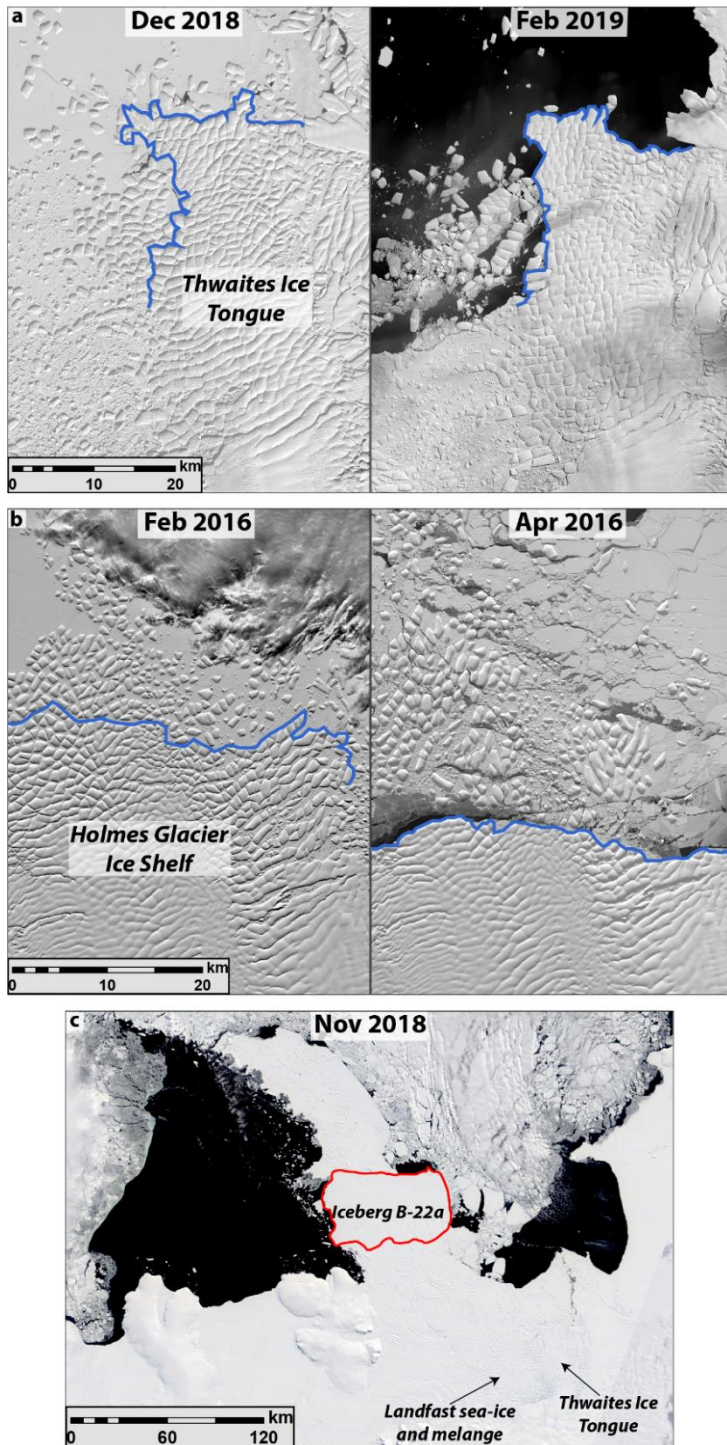


659

660 **Figure 6:** Sentinel-1 IW GRD images of the **a)** December 2015 - April 2016 calving event.

661 **b)** February – April 2017 calving event.

662



663

664

665

666

667

668

669

670

**Figure 7:** Landsat-8 images of Thwaites Glacier Tongue (a) and Holmes Glacier, Porpoise Bay, East Antarctica (b). Note their similarities and structure. Holmes Glacier disintegrates during landfast sea-ice break out events (e.g. Miles and others, 2017). A small portion of the Thwaites Glacier Tongue has disintegrated in response to a partial landfast sea-ice break out. Ice-fronts are digitized in blue. c) A MODIS image of the Amundsen Sea embayment. Note the grounded B-22A iceberg (digitized in red) and the dense landfast sea-ice which is anchored on to it.